

Reasonable Completed State and Parameter Analysis of a Double-Deck Steel Truss Arch Bridge

Zhengyang Zou¹, Jiahui Shan², Jishen Sun¹, Zuqian Jiang¹, Bin Sun^{1,*} and Rucheng Xiao¹

¹ Department, College of Civil Engineering, Tongji University, Shanghai 200092, China;

² CCCC Highway Consultants Co., Ltd., Beijing 100010, China.

* Correspondence: sunbin@tongji.edu.cn

Abstract: Double-deck arch bridges are increasingly used to accommodate rising traffic volumes due to their excellent mechanical properties, ease of construction, and economic benefits. However, research on double-deck steel truss arch bridges is insufficient, particularly regarding the influence of various design parameters on structural performance. This study focuses on a large-span double-deck steel truss arch bridge as the research object. First, the cable force distributions and the effectiveness of the completed bridge state obtained from four different cable force optimization methods, analyzing the differences between these methods and identifying the most suitable approach for achieving an optimal bridge completed state. Next, it further studies the effects on the structure caused by changes in parameters such as the ratio of side span to mid-span, the height of the main beam truss, and the height of the main arch truss, and deeply discusses the mechanical mechanisms. Finally, it summarizes the patterns observed, providing a reference for the design of similar engineering projects.

Keywords: steel truss arch bridge; dual-layer traffic; reasonable completed bridge state; cable force optimization; parameter analysis

Citation: Zou, Z.; Shan, J.; Sun, J.; Jiang, Z.; Sun, B.; Xiao, R. Reasonable Completed State and Parameter Analysis of a Double-Deck Steel Truss Arch Bridge. *Prestress Technology* 2024, 4, 43-53. <https://doi.org/10.59238/j.pt.2024.04.003>

Received: 14/11/2024

Accepted: 20/12/2024

Published: 30/12/2024

Publisher's Note: Prestress technology stays neutral with regard to jurisdictional claims in published maps and institutional affiliations.



Copyright: © 2024 by the authors. Submitted for possible open access publication under the terms and conditions of the Creative Commons Attribution (CC BY) license (<https://creativecommons.org/licenses/by/4.0/>).

1 Introduction

Arch bridges are a time-honored and structurally diverse bridge system that play a vital role in global bridge engineering [1]. Among the types of arch bridges, steel truss arch bridges are widely employed in large-span bridge projects, especially in areas with favorable geological conditions and high seismic demands. Their advantages include aesthetic appearance, large spanning capability, significant stiffness, and high stability [2]. Notable examples include the Chaotianmen Bridge (with a main span of 552 m), the Zigui Yangtze River Bridge (main span of 519 m), and the Nuijiang Bridge (with a main span of 490 m) [3-7].

To address the growing problem of single-layer traffic on large cross-river bridges, dual-layer traffic bridges have become increasingly common. This trend has driven the construction of more double-deck steel truss arch bridges, such as the Nanping Bridge in Zhuhai [8] and the Mingzhu Bay Bridge in Guangzhou [9]. Compared to traditional single-layer bridges, double-deck steel truss arch bridges offer superior structural performance, including greater stiffness and stability, increased spanning capabilities, and more flexible traffic capacity [10]. In recent years, domestic and international research has focused on the design, construction, and dynamic characteristics of double-deck truss arch bridges. For example, Guo et al. explored truss form selection, side and mid-truss dimensions, internal force adjustments, and the wind resistance of suspension rods during the design process of the Nanping Bridge [11]. Liu et al. evaluated the dynamic characteristics of the Mingzhu Bay Bridge structure by comparing measured values from field testing with theoretical values [12]. Zhang et al. discussed the key construction technologies for a double-deck bridge with a main span of 153 m, analyzing the detailed construction processes and corresponding critical control factors [13]. Li et al. studied the design concepts

of the Jinsha dual-purpose highway–railway bridge and provided a detailed commentary on the construction process [14]. Shao et al. investigated the use of ultrahigh-performance concrete in arch bridge structures and design concepts for kilometer-class arch bridges [15].

During bridge design process, appropriate structural parameters can better usage material performance, significantly impacting the safety and economy of the bridge. However, existing research has yet to fully address how parameter changes influence the mechanical responses of double deck steel truss arch bridges at different locations. Building on this research background, this paper examines the impact of changes in critical structural parameters on double-deck steel truss arch bridges, focusing on large span constructions. Firstly, this paper compares the cable force distribution patterns derived from different cable force optimization methods and evaluates the moments of the main beam and main arch under cable forces and dead loads, selecting the most suitable cable force optimization method for achieving a reasonable completed bridge state. secondly, three critical structural parameters were selected for study: the side-to-middle span ratio, the height of the main beam truss, and the height of the main arch truss. The changes in internal forces, displacements, and reactions of the structure were examined as these parameters changed, and the patterns and principles underlying these changes were analyzed.

2 Background Engineering Overview

In this work, a large-span double-deck steel truss arch bridge is taken as an object of study. The bridge features a continuous support structure with three spans and a bottom-bearing truss arch-beam combination. The span arrangement is 69 m + 162 m + 69 m. Both the arch and the girder are entirely constructed of steel, and the bridge features a double-layer deck layout, with both the upper and lower decks serving as six-lane urban expressways in both directions. Two main truss girders are arranged transversely with a spacing of 32.5 m, a center truss girder height of 9.3 m, and a node spacing of 9 m. High-strength parallel steel wire cables and high-strength alloy steel rods are used for suspension cables. The overall layout of the bridge is shown in **Figure 1**, and the finite element model is shown in **Figure 2**.

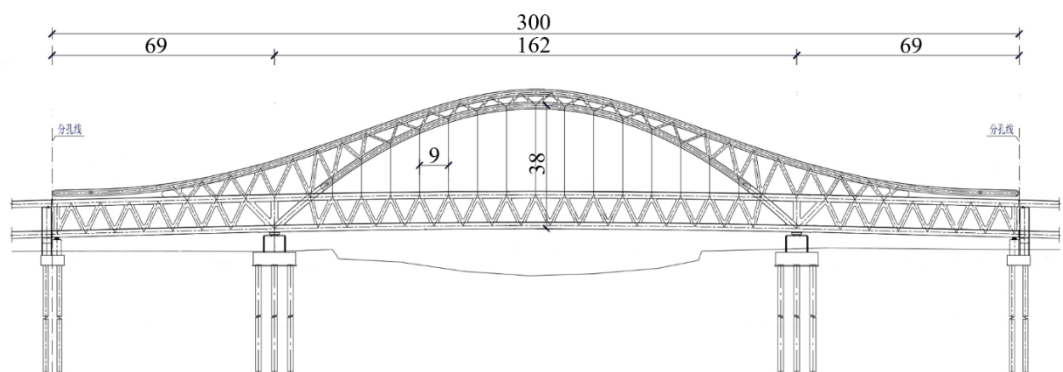


Figure 1 Overall layout of the main bridge (Unit: m)

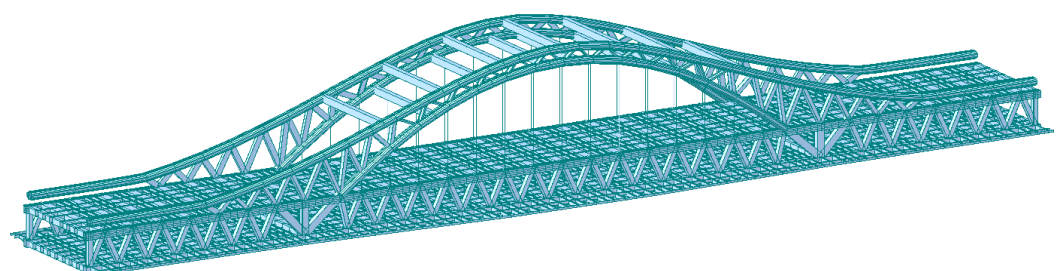


Figure 2 Finite element model of the main bridge

3 Determination of the Reasonable Completed Bridge Stage

In a double-deck steel truss arch bridge, cables are crucial load-bearing components. The magnitude of the cable force significantly affects the stress distribution throughout the entire structure. Therefore, optimizing the cable force during design helps adjust the stress state, bringing it closer to the desired completed bridge state. The rigid support continuous beam method and the zero-displacement method [16] are traditional approaches for cable force optimization. The former treats the main beam to a continuous beam, calculating the cable forces based on support reactions, whereas the latter iteratively adjusts the cable forces to minimize displacements at critical nodes of the main beam towards zero. The rigid hazard method follows a principle similar to the rigid support continuous beam method, optimizing cable forces by increasing the stiffness of the hangers. The minimum bending strain energy method [17], which is more commonly used, frames the determination of cable forces as an optimization problem aiming at minimizing the bending moment energy of the main beam to achieve a more balanced moment distribution.

During the design process, these four methods were used to calculate and optimize the cable forces for the suspension cables in the completed bridge state. The moment values of the main trusses and arch ribs under dead load and cable forces were calculated, and the results from the different optimization methods were compared. The structure includes a total of 15 suspension cables, numbered from left to right as D1 through D15.

The calculated tensile forces of the cables are shown in Figure 3. The figure reveals that the differences among the four methods are minimal, with the overall cable tension force obtained via the rigid hanger method being relatively small. The side hanger cable forces are higher in the rigid support continuous beam and rigid hanger methods, whereas the minimum bending strain energy method produces a more uniform cable force.

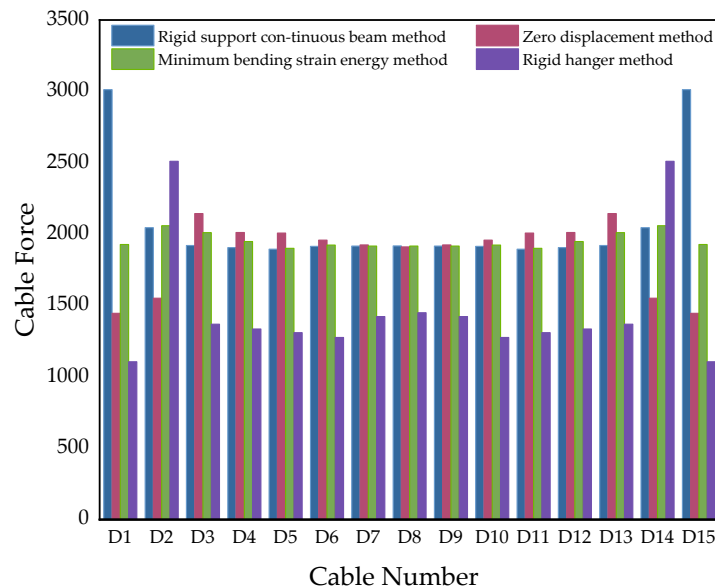


Figure 3 Cable force at the completed bridge stage

As shown in Figures 4 and 5, the main beam bending moment and arch bending moment under the action of a dead load, calculated using each of the four methods, are similar. The variation patterns of bending moments for both the upper chord and lower chord on the main beam also follow similar trends, with maximum positive and negative bending moments occurring at the arch foot, where there is a sudden change in the bending moment value. The overall bending moment variation of the arch rib also follows a consistent pattern. The middle span exhibits a relatively

uniform bending moment distribution, with the largest positive bending moment occurring at the connection between the top chord of the arch rib and the main truss, and the largest negative bending moment occurring at the arch foot. There is little variation in the maximum positive bending moment and maximum negative bending moment for the main beam and arch ribs obtained using different methods.

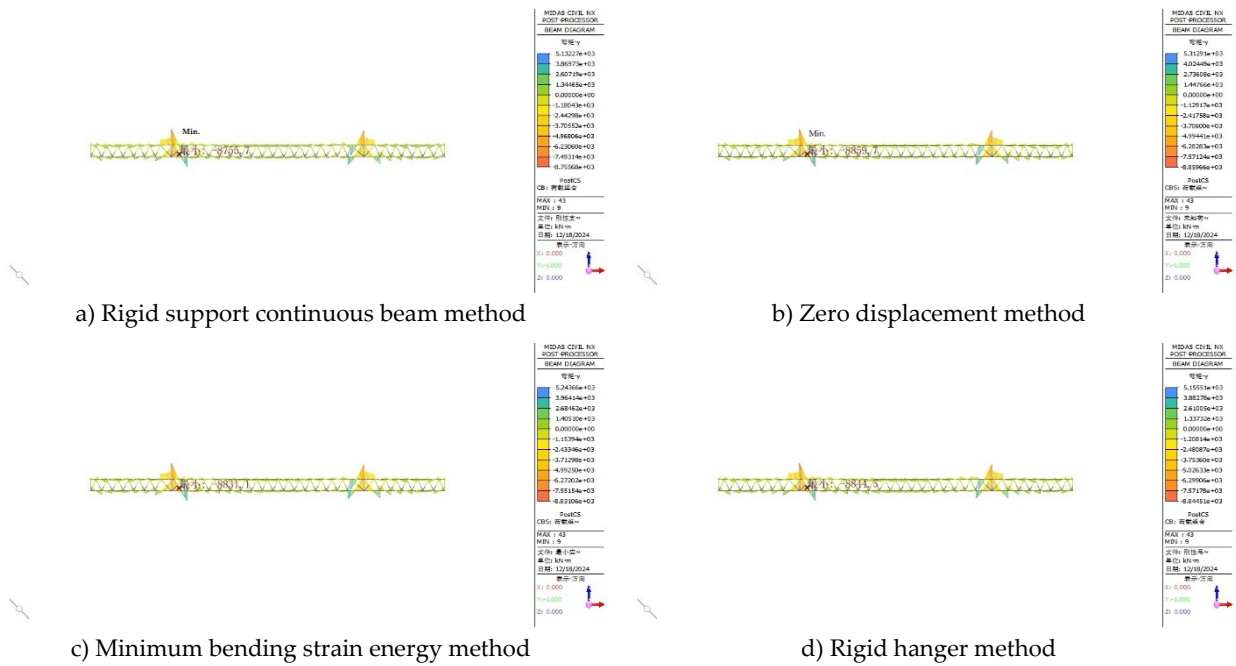


Figure 4 Bending moment of the main beam for different cable force optimization methods

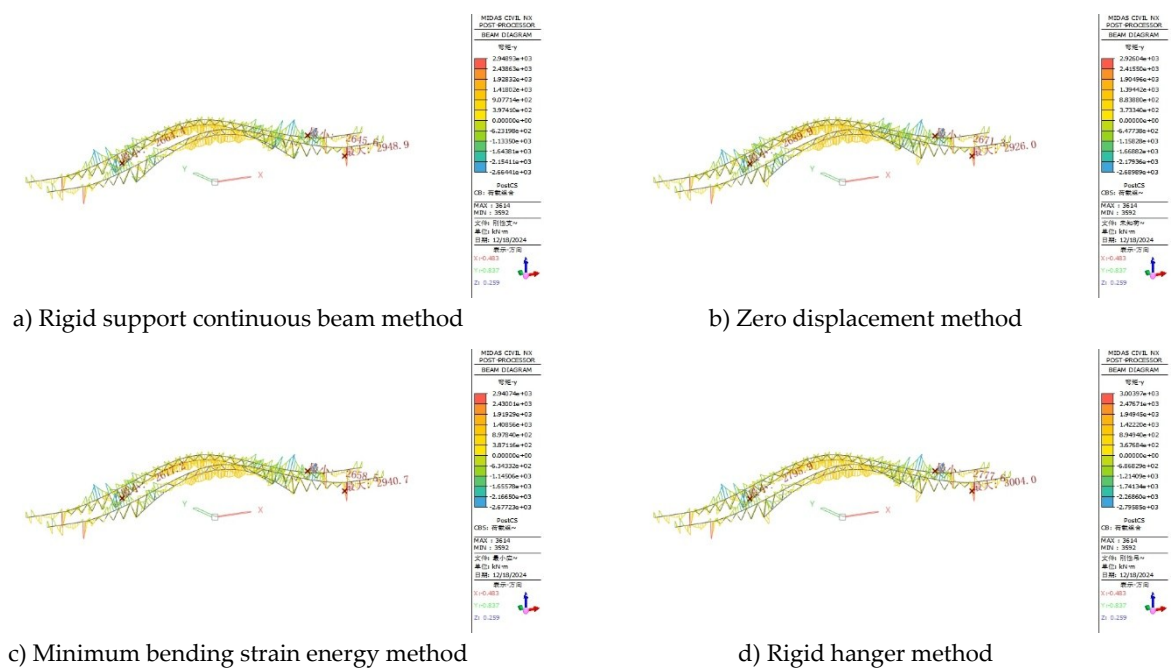


Figure 5 Bending moment of main arch ribs for different cable force optimization methods

Table 1 Comparison of main beam and main arch rib bending moment results (Unit: kN-m)

Cable force optimization method	Max. bending moment of main beam	Max. negative bending moment of main beam	Max. bending moment of main arch	Max. negative bending moment of main arch
Rigid support continuous beam method	5132.27	-8755.68	2948.93	-2644.41

Cable force optimization method	Max. bending moment of main beam	Max. negative bending moment of main beam	Max. bending moment of main arch	Max. negative bending moment of main arch
Zero-displacement method	5312.91	-8859.66	2926.04	-2689.89
Minimum bending strain energy method	5243.66	-8831.06	2940.74	-2677.23
Rigid hanger method	5155.51	-8844.51	3038.94	-2879.2

Overall, the cable force values obtained from the four different cable force optimization methods also show minimal differences. The main beam and arch ribs exhibit high stiffness and sufficient load-bearing capacity. The bending moments induced by loads are distributed according to their stiffness between the main truss and the arch rib. As shown in Table 1, variations in the cable forces do not significantly affect the structural stress state. However, the cable forces determined via the minimum bending strain energy method are the most uniform compared to the other methods. The other methods produce significant imbalances in the side hanger cable force values compared to those at other positions. Given these findings, it is recommended to prioritize the minimum bending strain energy method for cable force design during the actual design process.

4 Parameter Analysis of the Bridge Structure

The side-to-middle span ratio is typically determined during the conceptual design stage by considering factors such as terrain, geological conditions, navigation requirements, and construction convenience at the bridge site. The value of this ratio impacts the structural loading distribution. Analyzing its influence on the load-bearing capacity of a structure helps identify measures that are needed to maintain structural integrity and stability [1]. Furthermore, the height of the main beams and arches significantly influences the overall mechanical performance of structures. Variations in height alter stiffness ratios between the arches and beams, affecting load distribution and potentially causing substantial changes in the internal member forces, which could compromise structural safety. Therefore, this section studies how varying the side-to-middle span ratios, main beam heights, and arch heights affect the mechanical properties of the structures, offering reference values for future engineering designs.

4.1 The Ratio of the Side Span to the Middle Span

In this section, the ratio of the side span to the middle span is adjusted by maintaining a constant middle span length and while incrementally the side span length. Table 2 presents eight sets of parameters for analysis:

Table 2 Parameter reference values for the ratio of side to middle spans

Length of side span (m)	Ratio of side to middle span	Length of side span (m)	Ratio of side-to-middle span
42	0.259	78	0.481
51	0.315	87	0.537
60	0.37	96	0.593
69	0.426	105	0.648

As the middle span structure remains unchanged, variations in the ratio of the side span to the middle span display a relatively minor impact on the cable forces, arch axis geometry, and arch rib stress distribution. However, they significantly

influence the internal forces and deformations of the top and bottom chord members of the main beam. The following section examines the effects of the ratio variation on the internal forces, support reactions, and structural deformation under dead and live loads.

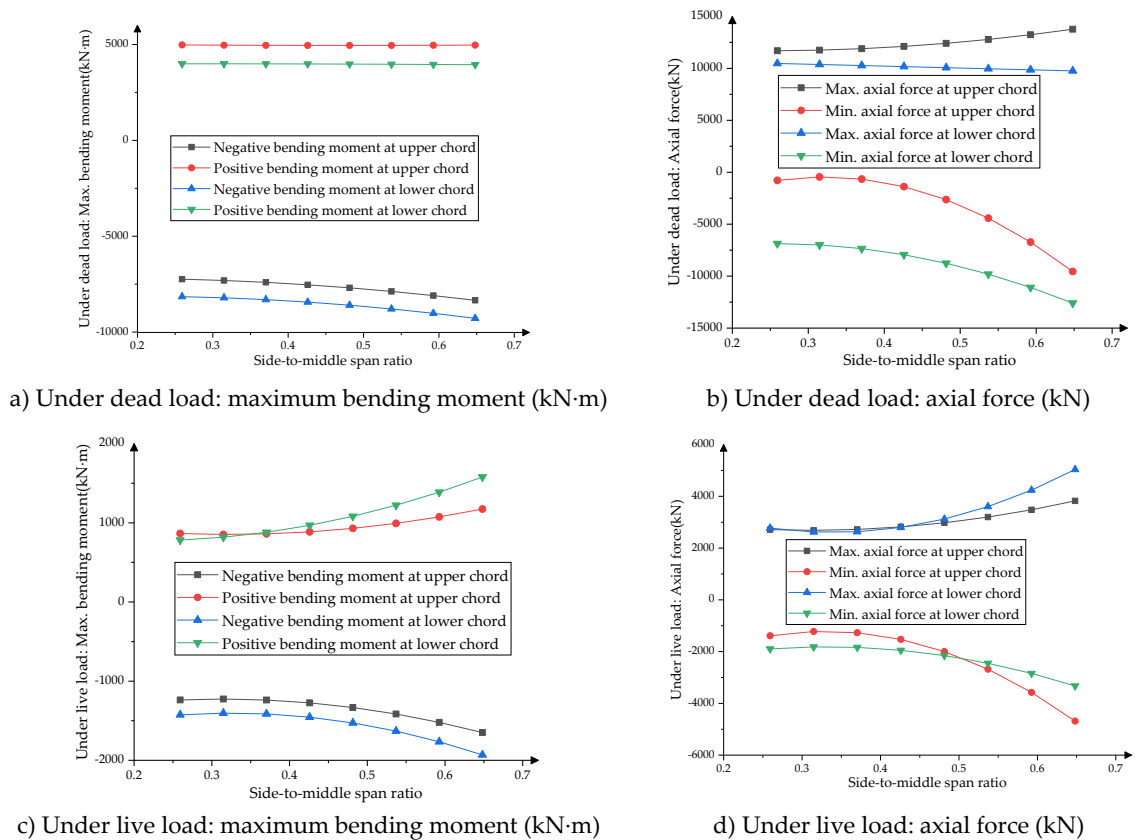


Figure 6 Influence of the side-to-middle span ratio on the main beam internal forces

Figure 6 illustrates the trends of the maximum positive and negative bending moments on the upper and lower chords of the main beam truss under dead and live loads. Under dead load, as the side-to-middle span ratio increases, the maximum positive moments in both the top and bottom chords of the main beam remain almost unchanged, whereas the maximum axial force gradually increases. Conversely, the maximum negative moment and the minimum axial force gradually decrease. Under live load, as the side-to-middle span ratio increases, the maximum positive moments and axial forces in both the top and bottom chords of the main beam gradually increase, whereas the maximum negative moment and the minimum axial force gradually decrease. Under live load, as the side-to-middle span ratio increases from 0.259 to 0.648, the maximum axial forces in the top and bottom chords of the main beam increase by 44% and 103%, respectively, while the minimum axial forces in the top and bottom chords decrease by 205% and 53%, respectively.

Figures 7 and 8 show the effects of the side-to-middle span ratio on the main beam deflection under live load conditions and the reaction force at the side support, respectively. As the ratio increases, the absolute values of the deflections gradually increase; however, since the main bridge uses a steel truss girder with high stiffness, even at the maximum value of 0.648 considered in this study, the stiffnesses of both sides still meet the specification requirements and have considerable excess capacity. Therefore, structural stiffness was not found to be controlled by the side-to-middle span ratio. Notably, when the ratio exceeds 0.5, the beam deflection due to live loads rapidly increases, which should be considered during design. The minimum reaction forces at the side support also increase with higher ratios, but their growth rate decreases gradually. Among all the ratios tested, only when the ratio was 0.259 did the side support experience negative reactions.

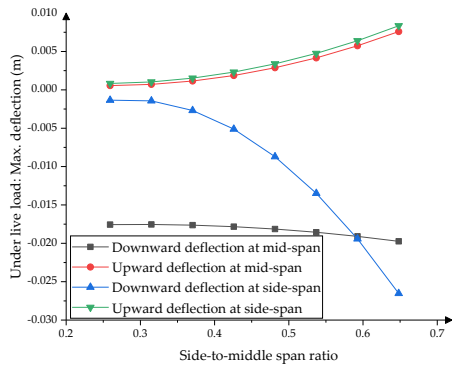


Figure 7 Beam deflection under live load conditions at different side-to-middle span ratios

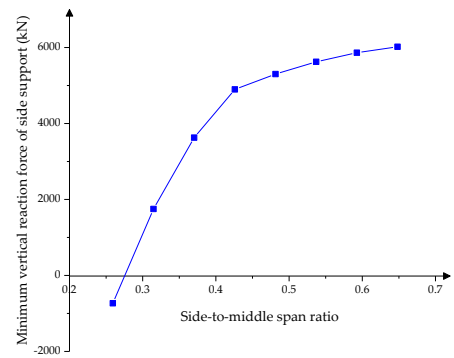


Figure 8 Side support reactions at different side-to-middle span ratios

In summary, determining a reasonable value of the side-to-middle span ratio for a double-deck steel truss arch bridge should consider the following factors: (1) the length of the side span must ensure that, even in the most unfavorable load arrangement, no negative reaction force appears at the side support. Therefore, the ratio of the side span to the middle span should be greater than 0.3. (2) For a double-deck steel truss arch bridge, the side-to-middle span ratio primarily affects the upper and lower chord axial forces of the side span during the design process, so special attention needs to be paid to this in the design process. In subsequent studies, the aforementioned patterns will be further validated in other double-deck truss arch bridges.

4.2 Height of the Main Beam

The effects of beam height variation ranging from 7.5 m to 12.5 m, with a baseline value of 9.5 m, are shown in Table 3. Since increasing the truss height only slightly increases the length of the web members, the structural weight changes by less than 0.1%, and the impact on suspension cables tension force is minimal. Therefore, this section continues to use the original cable forces for subsequent analysis.

Table 3 Parameter values of the main beam truss height

Truss beam height (m)	Rate of change	Truss beam height (m)	Rate of change
7.5	79%	10.5	111%
8.5	89%	11.5	121%
9.5	100%	12.5	132%

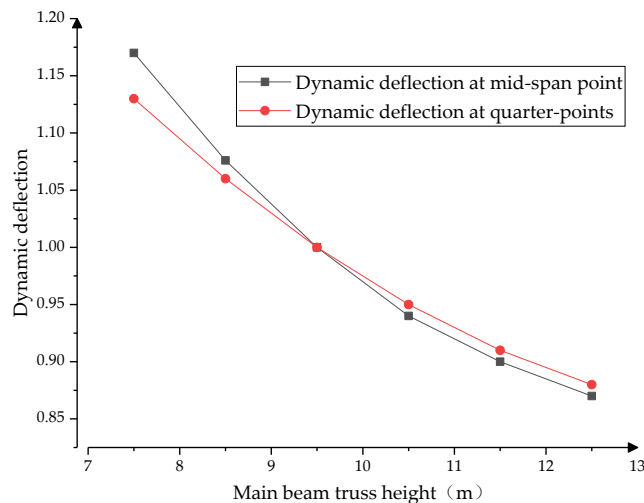


Figure 9 Variation in overall stiffness with truss beam height

When the height of the main beam truss changes, the structural stiffness also changes. In this section, the dynamic deflection at the mid-span point and quarter-points of the main beam are selected as representative values for overall stiffness. These deflections are normalized by dividing them by the original design's dynamic deflection to study how the change in the heights of the main beam and main arch truss affect the overall stiffness of the structure. Figure 9 shows the impact of changing the main beam truss height on the overall stiffness. Increasing the main beam truss height leads to an improvement in the overall stiffness. However, this enhancement is limited, as the originally designed double-deck truss bridge already functions as a rigid frame–rigid arch system with significant initial stiffness.

To study the influence of changes in the height of the main beam truss on the distribution of internal forces, 22 representative members at various critical locations were selected: midspan points, quarter points, intersection points of the arch and beam, and side span positions, both on the main beam and the main arch. This selection aims to study the height variation effect on member axial forces at different locations.

As shown in Figure 10, under live load action, an increase in height of the main results in longer arm lengths for the upper and lower chord members inside the main beam. Therefore, the axial force required to produce the same bending moment decreases, resulting in a reduction in the axial forces for all components of the main beam and arch. Additionally, the rate of change for each component is uniform and less than 50% on average when subjected to live loads. This is because the majority of the live load distribution between arches occurs through hangers, with only a small portion transferred through the junctions of the beam and arch. Consequently, when the stiffness ratio of the arch beams is altered, the redistribution of live loads along different longitudinal positions becomes more even rather than being concentrated on only a few components.

Notably, when the main beam truss height is increased while maintaining a constant spacing of main beam nodes, the horizontal angle of the web bars increases. This leads to higher internal forces at the intersection between the main beam and main arch, which can negatively affect the stability of the web bar at these points.

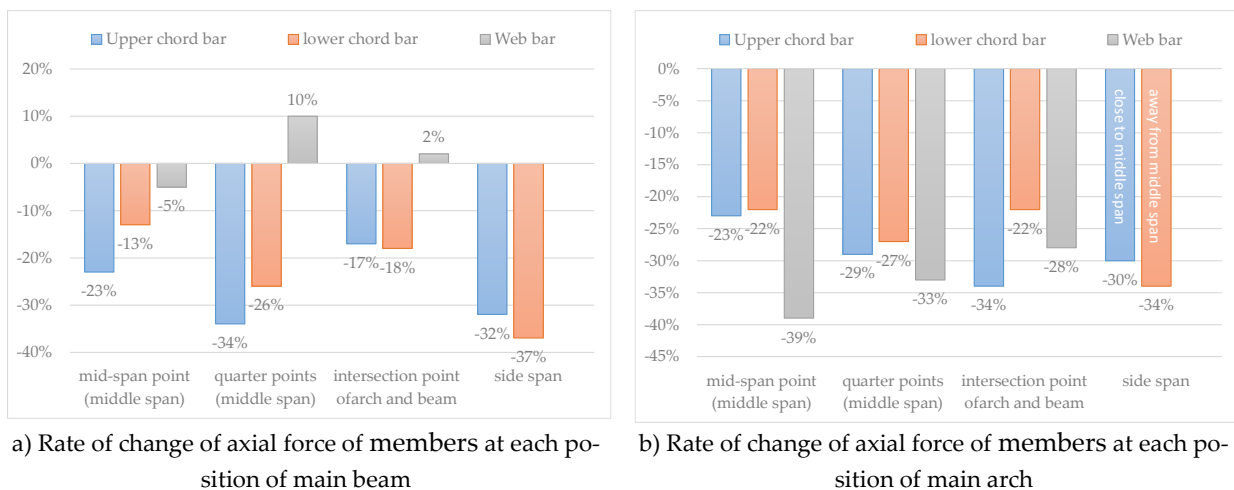


Figure 10 Effects of variations in the main beam truss height on the axial forces of the members

4.3 Height of the Main Arch Truss

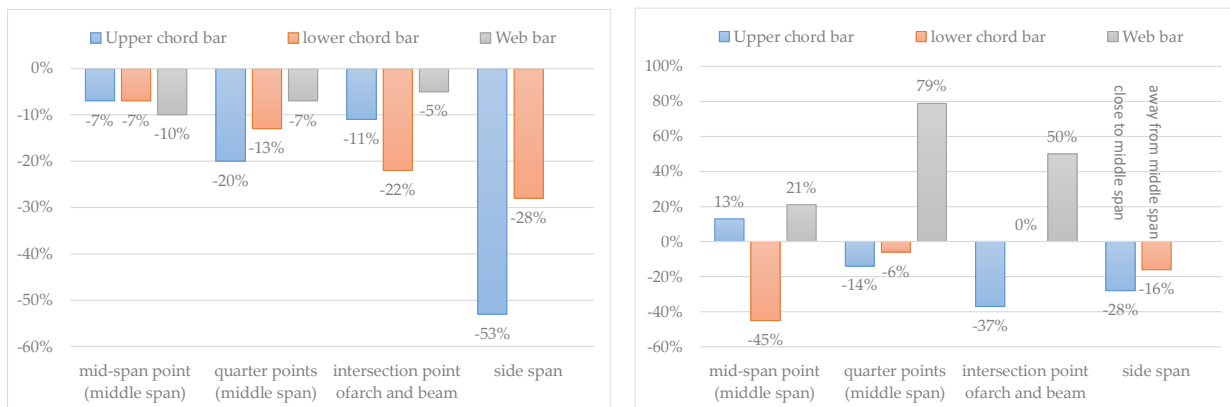
Like in the previous chapter, this section considers the main arch truss height with an arch crown height of 3.85 m. The arch height varies from 1.85 m to 6.85 m, as shown in Table 4. The members studied are the same as those in Section 4.2.

Table 4 Parameter values of the main arch truss height

Truss height of arch (m)	Rate of change	Truss height of arch (m)	Rate of change
1.85	48%	4.85	126%
2.85	74%	5.85	152%
3.85	100%	6.85	178%

Since the original design of the double-deck truss arch bridge is a rigid beam and rigid arch system, changes in the main arch truss height result in only minimal changes in structural rigidity. Therefore, this aspect will not be further elaborated here.

According to Figure 11, under live load action, the axial forces of all the members decreases as the main arch truss height increases. This trend follows the same reasoning as discussed in the previous chapter. Among these values, the change rate of the mid-span members is relatively low, whereas the change rate near the intersection between the arch beam and the main beam is greater. This is due to the localized internal force distribution at the junction between the main arch and the main beam. The axial forces in most of the upper and lower chords of the main arch decreased, whereas the axial forces in the web bars increased. Notably, the axial compressive force in the web bars at the quarter points of the main arch increased by 79%. The increase in the length of the web bars and their axial compressive forces is detrimental to the stability of these members.



a) Rate of change of axial force of members at each position of main beam

b) Rate of change of axial force of members at each position of main arch

Figure 11 Effect of variations in the main arch truss height on the axial force of the members

5 Conclusions

Through research on the optimal construction state and structural parameters of double-deck steel truss arch bridges, we summarize the following insights for future design of similar bridges:

The differences in the optimized cable force obtained by different optimization methods are minimal, primarily affecting the side hangers and uniformity. However, the internal forces of the main beam and arch ribs after optimization are very similar.

The side-to-middle span ratio should be greater than 0.3 to prevent negative reaction forces at the side support. Additionally, special attention should be given to the axial forces in the upper and lower chords of the main beam on both sides when designing the side-to-middle span ratio.

Increasing the height of the main beam truss reduces most of the axial forces in the main beam and arch, but it increases the length and axial force of the web bars at

the intersection between the arch and the beam. Special attention should be given to the stability of the web bars at this point.

Increasing the height of the main arch truss also reduces most of the axial forces in the main beam and arch, with greater changes in the axial force at the intersection between the arch and the beam. Since both the length of the web bars and their axial compressive forces have increased, this is detrimental to the stability of those members.

Conflict of interest: All the authors disclosed no relevant relationships.

Data availability statement: The data that support the findings of this study are available from the corresponding author, Sun, upon reasonable request.

Funding: The authors appreciate the support from the Department of Transportation of Zhejiang Province under grant No. 2021060.

References

1. Xiao, R. *Bridge Structural System*; China Communications Press: Beijing, 2013.
2. Sun, H. Research on Key Problems of Large-Span Steel Truss Arch Bridges. Ph.D., Tongji University, 2006.
3. Wang, F.; Xu, W. Study on Structural System of Main Bridge of Chongqing Chaotianmen Yangtze River Bridge. *Technology of Highway and Transport* **2005**, 23-28, doi:10.3969/j.issn.1009-6477.2005.z1.005.
4. Xu, X.; Jiang, B.; Chen, K. Key Construction Techniques for Main Bridge of Zigui Changjiang River Highway Bridge. *World Bridges* **2023**, 51, 55-62, doi:10.20052/j.issn.1671-7767.2023.S1.009.
5. Ding, W.; Du, Y.; Jiang, L. Comprehensive Survey Technology and Result Analysis of the Four-line Long-span Nu River Station Bridge in Dali-Ruili Railway. *Railway Standard Design* **2018**, 62, 101-106, doi:10.13238/j.issn.1004-2954.201705110005.
6. Zhou, X.; Zhang, X. Thoughts on the Development of Bridge Technology in China. *Engineering* **2019**, 5, 1120-1130.
7. Wang, G.; Ding, Y. Research on monitoring temperature difference from cross sections of steel truss arch girder of Dashengguan Yangtze Bridge. *International Journal of Steel Structures* **2015**, 15, 647-660, doi:10.1007/s13296-015-9011-9.
8. He, J.; Guo, J.; Gao, K. Static Dynamic Analysis of Double-Deck Steel Truss Arch Bridge—Nanping Bridge Engineering Design. *Urban Roads Bridges & Flood Control* **2015**, 59-62, doi:10.3969/j.issn.1009-7716.2015.07.019.
9. Shanguan, B.; Hu, H.; Zhao, J.; An, L. Key Technologies for Structural System Design of Mingzhu Bay Bridge in Guangzhou. *Bridge Construction* **2022**, 52, 1-7, doi:10.3969/j.issn.1003-4722.2022.04.001.
10. Li, M.; Sun, Y.; Lei, Y.; Liao, H.; Li, M. Experimental Study of the Nonlinear Torsional Flutter of a Long-Span Suspension Bridge with a Double-Deck Truss Girder. *International Journal of Structural Stability and Dynamics* **2021**, 21, doi:10.1142/s0219455421501029.
11. Guo, J.; Du, J.; Gao, K. Discussion on the Design of Double-Deck Steel Truss Arch Bridge of Nanping Bridge. *Urban Roads Bridges & Flood Control* **2017**, 65-67, doi:10.16799/j.cnki.csdqyf.2017.01.018.
12. Liu, W.; Zhang, P.; Zhong, X.; Zhao, Z.; Qiao, S. Research on Modal Parameter Identification of Double Deck Half-through Continuous Rigid Truss Arch Bridge Under Environmental Excitation. *Guangzhou Architecture* **2023**, 51, 33-36, doi:10.3969/j.issn.1671-2439.2023.05.009.
13. Zhang, K.; Hou, F.; Liu, X. Key Technology for Construction of Double-deck Steel Truss Arch Bridge for Highway and Railway Use. *Urban Roads Bridges & Flood Control* **2023**, 140-142, doi:10.16799/j.cnki.csdqyf.2023.05.036.
14. Li, Y.; Li, H.; Xu, B. Jinsha River Bridge, China: the World's First Double-Deck Road and High-Speed Railway Arch Bridge. *Proceedings of the Institution of Civil Engineers. Bridge engineering* **2020**, 173, 179-189, doi:10.1680/jbren.19.00031.
15. Shao, X.; He, G.; Shen, X.; Zhu, P.; Chen, Y. Conceptual Design of 1000 m Scale Steel-UHPFRC Composite Truss Arch Bridge. *Eng Struct* **2021**, 226, 111430.111431-111430.111412, doi:10.1016/j.engstruct.2020.111430.
16. Wang, Y.; Liu, S.; Tan, H.; Xiao, R. Theoretical Study on Optimization of Cable Force in Cable-stayed Bridge. *Highway* **2006**, 31-34, doi:10.3969/j.issn.0451-0712.2006.05.007.

17. Liang, P.; Xiao, R.; Zhagn, X. Practical Method of Optimization of Cable Tensions for Cable-stayed Bridges. *Journal of Tongji University(Natural Science)* **2003**, 31, 1270-1274, doi:10.3321/j.issn:0253-374X.2003.11.003.

AUTHOR BIOGRAPHIES

	<p>Zhengyang Zou M.E., Studying at Civil Engineering, Tongji University.</p> <p>Research Direction: Design of Bridge Structures.</p> <p>Email: bancroftzou@foxmail.com</p>		<p>Jiahui Shan M.E., Assistant Engineer. Working at CCCC Highway Consultants Co., Ltd.</p> <p>Research Direction: Research and Development of CAE Software.</p> <p>Email: 2132536@tongji.edu.cn</p>
	<p>Jishen Sun M.E., Studying at Civil Engineering, Tongji University.</p> <p>Research Direction: Design and Optimization of Long-span Bridges.</p> <p>Email: 2330631@tongji.edu.cn</p>		<p>Zuqian Jiang D.Eng, Studying at Civil Engineering, Tongji University.</p> <p>Research Direction: Risk Analysis and Quantification of Bridges.</p> <p>Email: zuqianjiang@tongji.edu.cn</p>
	<p>Bin Sun D.Eng, Associate Professor, Working at Civil Engineering, Tongji University.</p> <p>Research Direction: Bridge Structural System.</p> <p>Email: sunbin@tongji.edu.cn</p>		<p>Rucheng Xiao D.Eng, Professor, Working at Civil Engineering, Tongji University.</p> <p>Research Direction: Bridge Structural System.</p> <p>Email: xiaorc@tongji.edu.cn</p>